Introduction

In this lab, we were tasked with building a navigation stack using two sensors, a GPS and an IMU, to explore sensor fusion. Since we previously developed ROS2 drivers for both sensors in Labs 1 and 3, we were able to integrate them into to collect both GPS and IMU data. A new launch file was created to start both sensors at the same time.

Two different datasets were collected. The first was of a circular driving pattern around a roundabout, which was gathered to calibrate the magnetometer by analyzing hard and soft iron effects. The second dataset comprised a comprehensive 10-minute drive around Northeastern University, so we could attempt to map our route.

The primary focus of this lab was to understand the strengths and limitations of each sensor type while exploring methods of sensor fusion for improved navigation estimates. Our analysis examines three main areas: heading estimation through magnetometer calibration and sensor fusion, forward velocity estimation through both GPS and IMU data, and position estimation through dead reckoning techniques.

Jack Gladowsky driver was used to collect data for this lab.

Analysis

Estimating Yaw – Magnetometer Calibration

The magnetometer data was calibrated using both hard and soft iron corrections based on data collected while driving in circles. Hard iron effects, which result from permanent magnets and magnetized materials in the vehicle, were corrected by subtracting the mean offsets. Soft iron effects, caused by materials that distort the surrounding magnetic field, were corrected using the calculated correction matrix. As shown in the plots, the raw magnetometer data exhibited a clear circular pattern that was offset from the origin. After applying the hard iron correction, the data was centered at the origin, and the soft iron correction helped maintain the circular shape of the measurements.

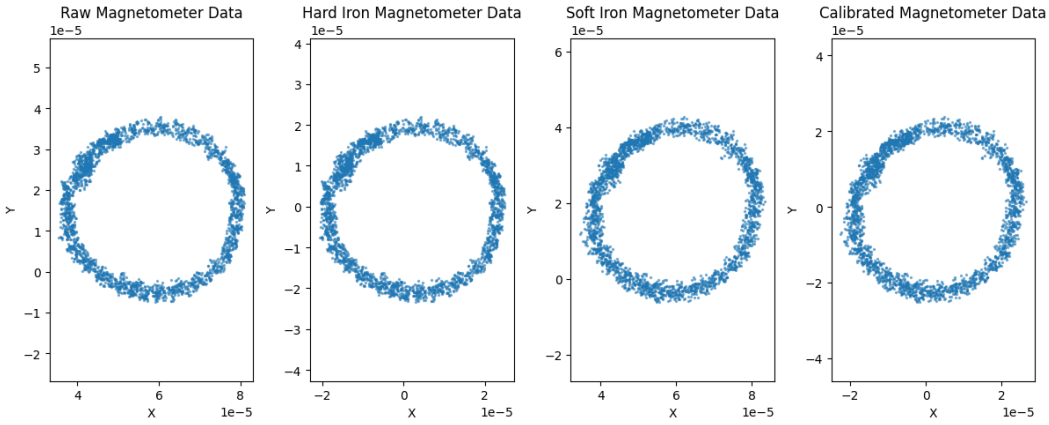

Figure 1. Magnetometer Calibration

We then used these offsets to correct our full driving data, the raw data vs the corrected data is shown in figure 2.

Figure 2

Estimating Yaw – Sensor Fusion

The yaw estimation analysis involved comparing three different methods, as shown in the figures. First, comparing the magnetometer-derived yaw with integrated gyroscope data revealed characteristics of each sensor. The magnetometer data showed more noise but maintained stable long-term readings, while the integrated gyroscope data exhibited smoother transitions but suffered from significant drift over time.

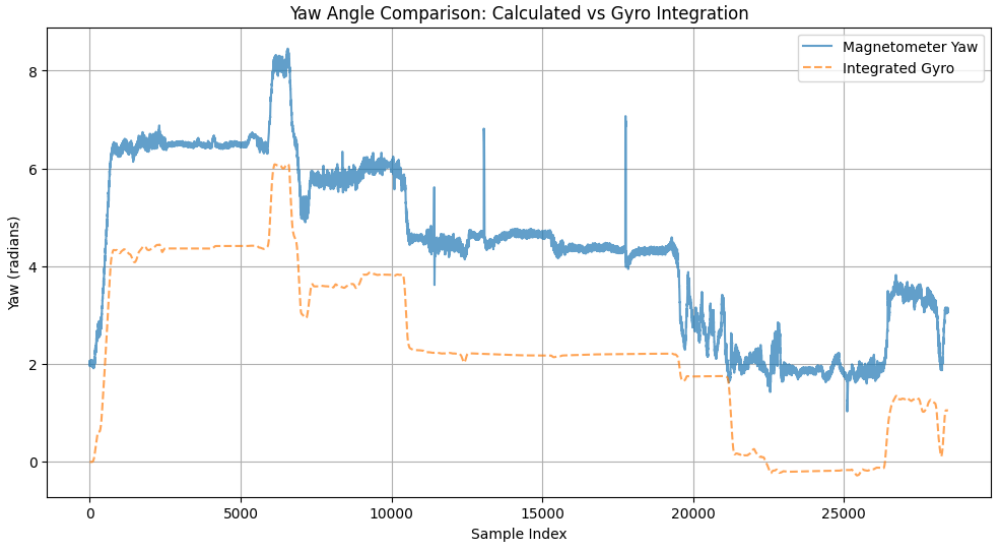

Figure 3

A complementary filter was implemented with α=0.95 to combine these measurements. As shown in the filter comparison plot, the low-pass filtered magnetometer data (green) and high-pass filtered gyroscope data (red) were combined to produce the final estimate (purple). The high alpha value heavily weighted the magnetometer data, effectively reducing gyroscope drift while maintaining responsiveness to heading changes.

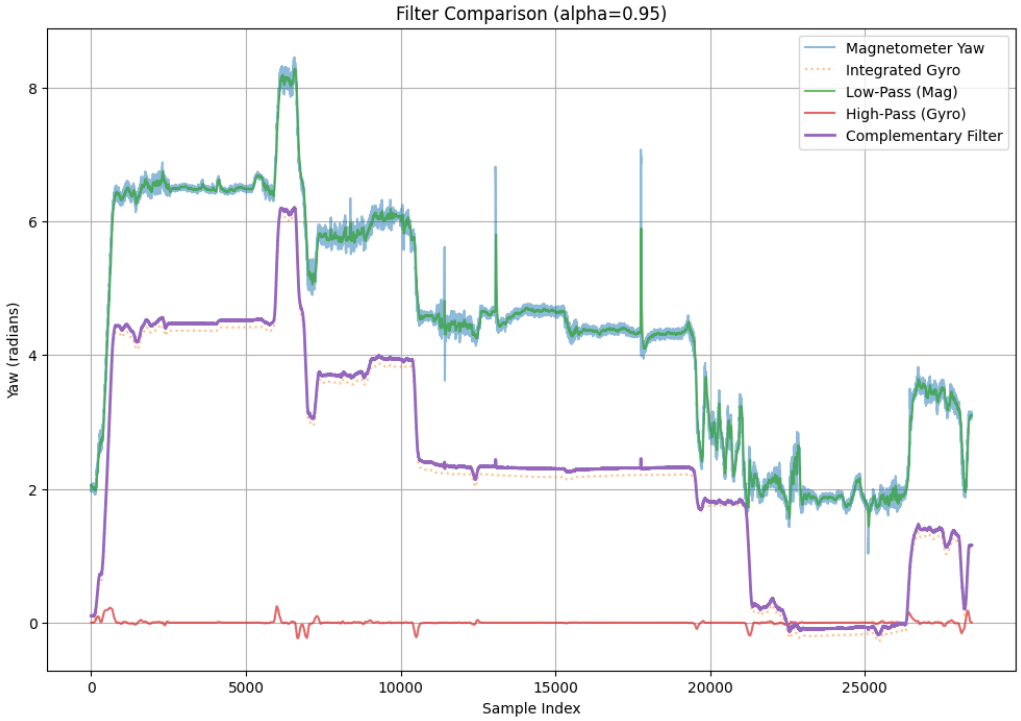

Figure 4

The final comparison between our complementary filter and the IMU's internal yaw computation demonstrated excellent agreement in tracking heading changes. The complementary filter successfully captured all major turns and maintained stability during straight segments, closely matching the IMU's built-in estimation. This confirms that the complementary filter would work well for navigation.

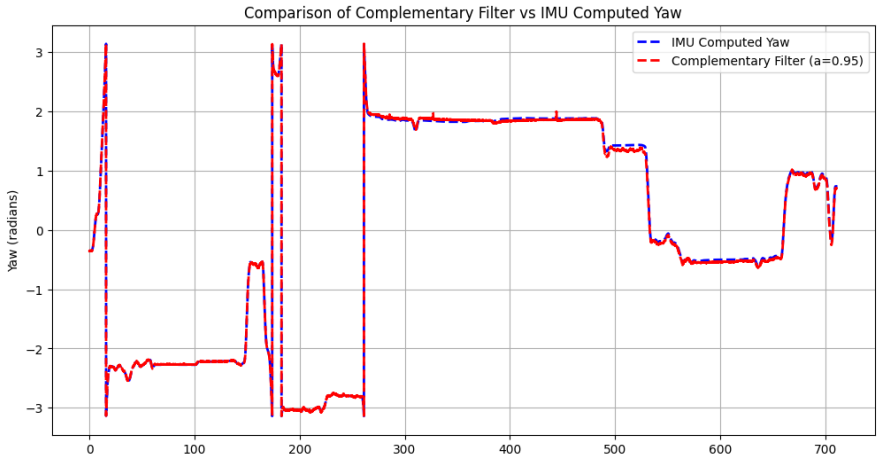

Figure 5

Estimating the Forward Velocity

The initial velocity estimation from integrating the raw accelerometer data showed significant drift, with the velocity continuously increasing to unrealistic values of up to 140 m/s. This drift was primarily due to accelerometer bias and integration errors. The GPS velocity provided a more realistic baseline, showing speeds consistent with urban driving. The unadjusted plot is shown in figure 6.

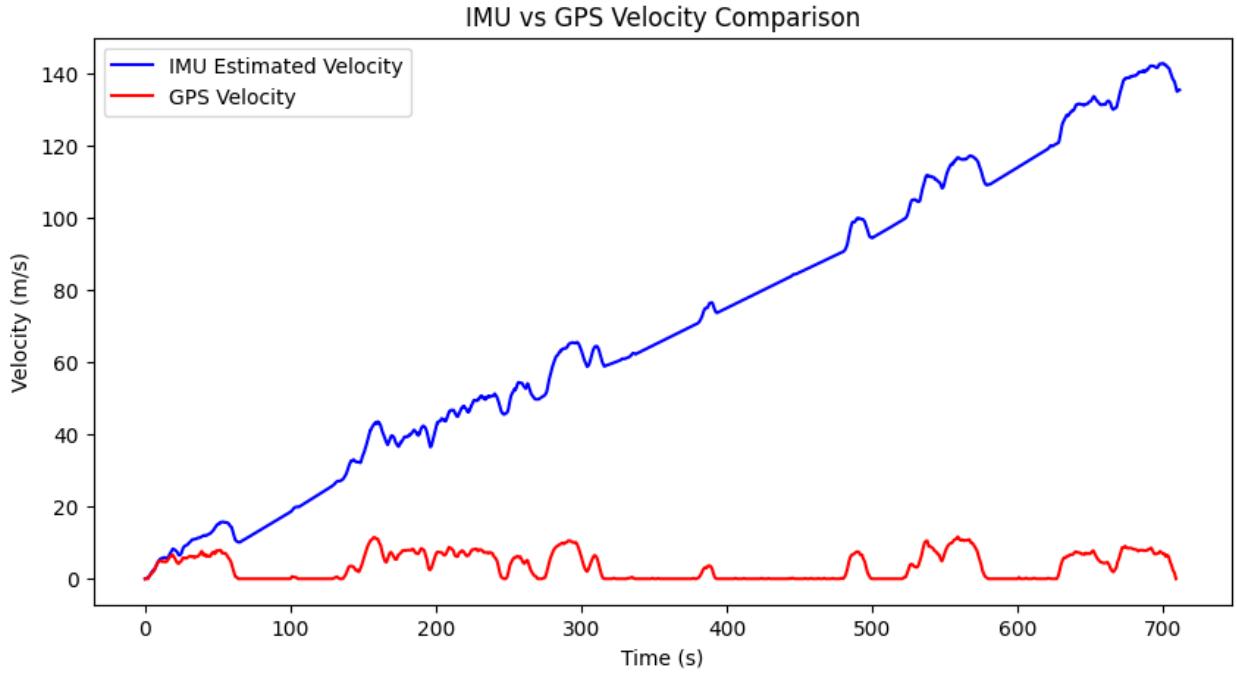

Figure 6

To improve the IMU-based velocity estimate, we first addressed the inherent bias in the accelerometer data by calculating and removing the mean acceleration from an initial 100-sample window. This raw signal was then smoothed using a Butterworth low-pass filter with a cutoff frequency of 0.5 Hz to reduce high-frequency noise while preserving the underlying motion characteristics. Small acceleration values (below 0.05 m/s^2) were then zeroed out to prevent drift during nearly stationary periods. Finally, after integration, we removed the linear trend from the velocity data to compensate for any remaining systematic bias.

The detrended shows much better agreement with the GPS velocity measurements. While some discrepancies remain, particularly during stops and rapid accelerations, the overall velocity profile now more accurately reflects the vehicle's motion. The remaining differences can be attributed to inherent sensor noise and the challenging nature of double integration for position estimation as shown in the imprecise magnitude and slopes of some parts. The detrended plot is shown in figure 7.

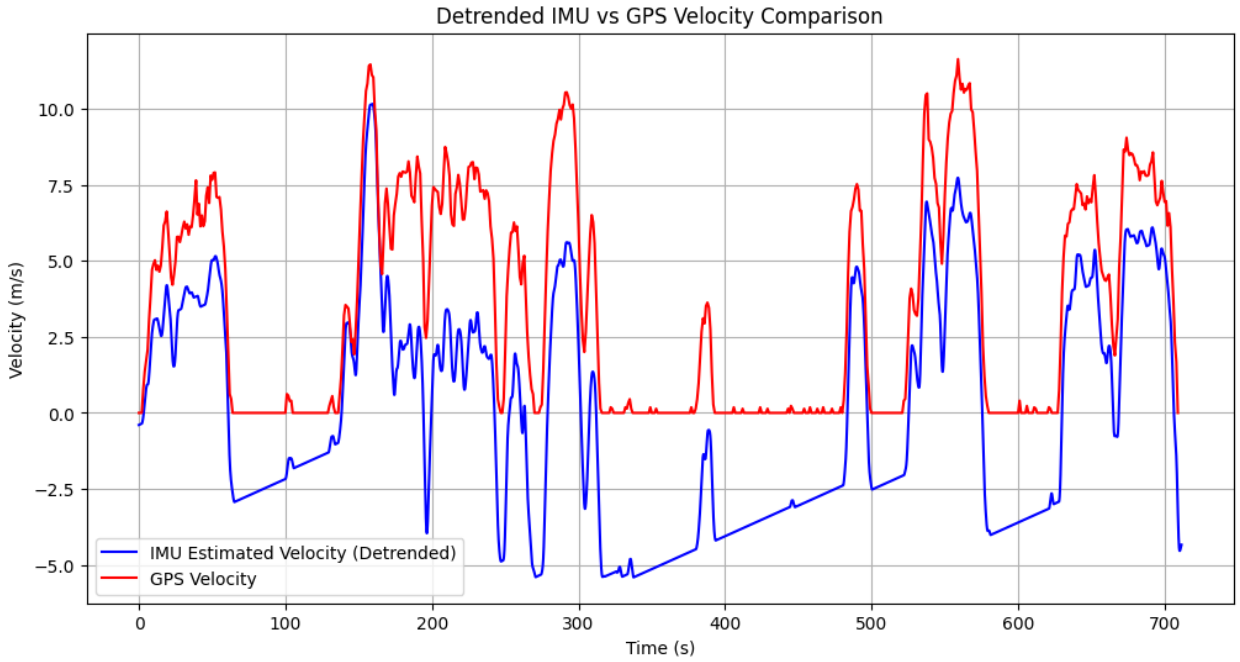

Figure 7

Dead Reckoning with IMU

The comparison between ωẊ and ÿ_obs shows similar patterns in acceleration during turns, but with notable magnitude differences. While both signals capture the major turning events, ÿ_obs consistently shows larger peaks, particularly around the 300-second mark. These differences likely arise from our simplifying assumptions, particularly setting xc = 0 (assuming the IMU is mounted at the center of mass) and assuming no lateral motion (Ẏ = 0). The plot is shown in figure 8 and shows that both plots follow similar general trends but have different magnitudes and smaller fluctuations.

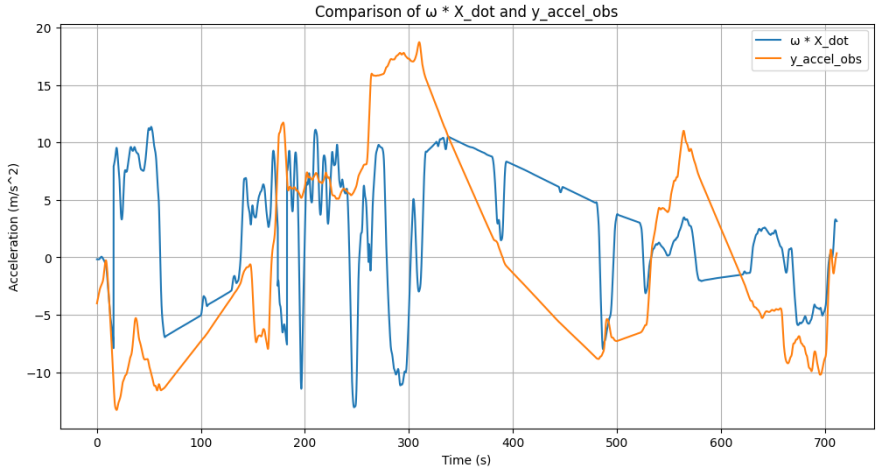

Figure 8

To properly align the IMU trajectory with GPS data, we first matched the starting positions of both paths to begin at the origin. Then, using the initial straight-line segment as a reference, we applied a rotation to align the IMU's heading frame with the GPS coordinate frame. This initial rotation corrected for the arbitrary zero-reference of the IMU's heading measurements relative to true north. Without this alignment step, the dead reckoning trajectory initially propagated in the wrong direction, as seen in figure 9. After applying the rotation correction (figure 10), the trajectory showed much better agreement with the GPS ground truth, particularly in the early segments of the drive. Although the dead reckoning did not closely show us the GPS trajectory, we still were able to get a general trajectory and can see some similarities between the two plots as in the lengths and angles of some of the paths.

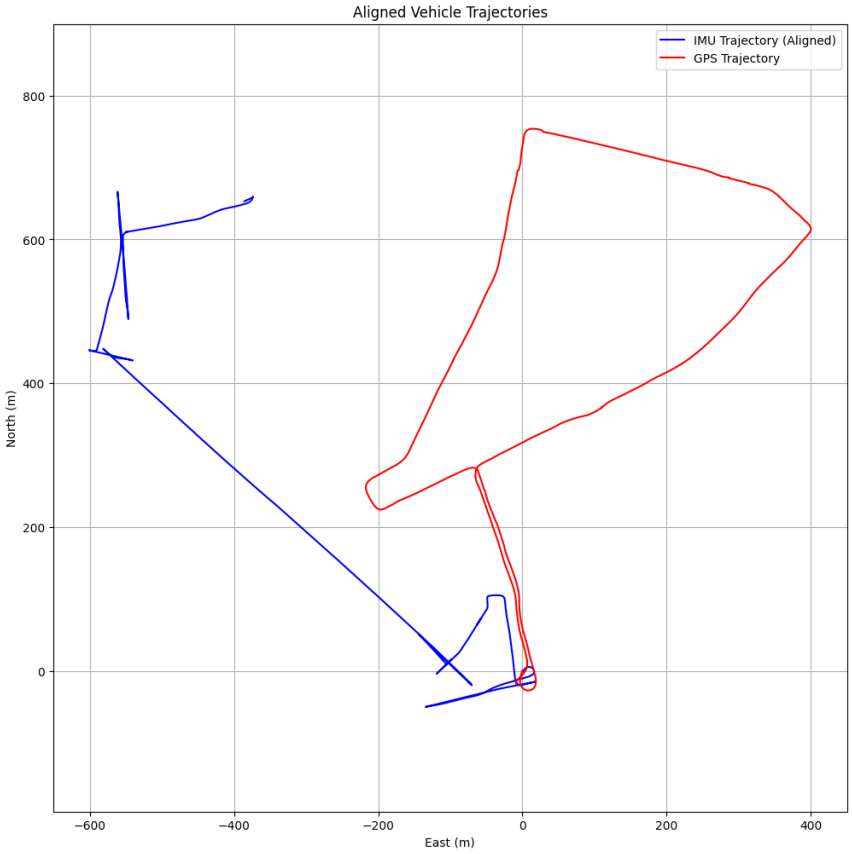

Figure 9

However, the dead reckoning solution still accumulated significant drift over time, with errors growing more pronounced during and after turns. This behavior aligns with expected limitations of IMU-based dead reckoning, where small errors in velocity and heading compound during integration. Based on this dataset, the IMU trajectory maintained reasonable accuracy (within 2 meters of GPS) for approximately 30 seconds before significant drift became apparent, particularly in the north-south direction.

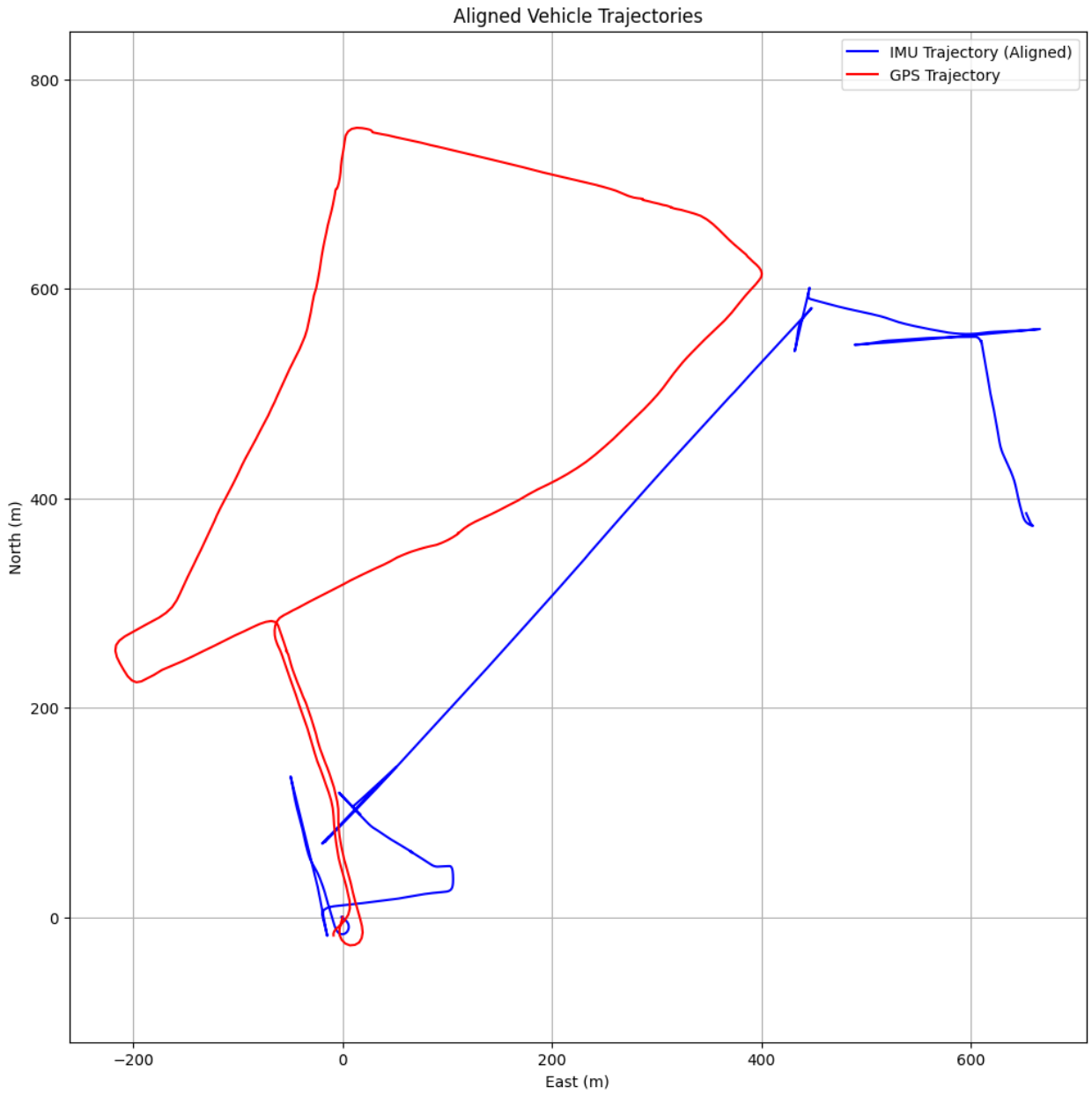
Aligned Vehicle Trajectories
IMU Trajectory (Aligned)
GPS Trajectory
North (m)
East (m)
800
600
400
200
0
−200
0
200
400
600

Figure 10

Results

Magnetometer Calibration Results

Our analysis of the magnetometer data revealed significant hard iron effects, with offsets of (5.608e-05, 1.592e-05, 4.671e-06). After hard iron correction, the data was centered at the origin. The soft iron correction matrix showed small distortion effects, with diagonal values close to 1 and small off-diagonal terms, which means the car did not affect the readings very much.

Heading Estimation Results

The complementary filter (α=0.95) successfully combined the stability of magnetometer measurements with the smoothness of gyroscope data. The magnetometer-derived heading provided long-term stability but exhibited noise, while the integrated gyroscope data showed smooth transitions but suffered from drift. The complementary filter effectively mitigated both issues, producing heading estimates that closely matched the IMU's computations while not using any accelerometer data.

Velocity Estimation Results

Integration of the IMU's accelerometer data revealed significant drift characteristics, with uncorrected estimates reaching physically impossible velocities over 140 m/s. To address these errors, we implemented a series of corrections. A 100-sample window was used to calculate and remove the initial accelerometer bias, followed by a Butterworth low-pass filter with 0.5 Hz cutoff to reduce high-frequency noise. Accelerations below 0.05 m/s² were zeroed to prevent small noise contributions from accumulating during integration. Finally, linear detrending was applied to the integrated velocity to compensate for residual systematic errors. Comparing ωẊ and ÿ_obs showed consistent temporal patterns during vehicle turns but revealed amplitude discrepancies, suggesting the presence of unmodeled dynamics in our simplified vehicle motion model.

Dead Reckoning Results

Dead reckoning analysis using the corrected velocity measurements and complementary filter heading estimates demonstrated the challenges of inertial navigation. Initial trajectory alignment required matching both starting positions and heading reference frames to see a comparison with GPS data. Even after these corrections, the IMU-derived trajectory-maintained accuracy within 2 meters of GPS measurements for at maximum about 30 seconds. Position errors accumulated rapidly, with heading inaccuracies causing significant drift during and after turning maneuvers. This degradation aligns with expectations for inertial navigation, where small errors in both velocity and heading estimates compound through the integration process. The results clearly demonstrate why modern navigation systems typically employ sensor fusion techniques rather than relying solely on inertial measurements for extended periods.